PHYSICAL REVIEW B **72**, 161404(R) (2005)

Fine structure of the radial breathing mode of double-wall carbon nanotubes

R. Pfeiffer,[1] F. Simon,[1] H. Kuzmany,[1] and V. N. Popov[2]
[1]*Institut für Materialphysik, Universität Wien, Strudlhofgasse 4, 1090 Wien, Austria*
[2]*Faculty of Physics, University of Sofia, Sofia, Bulgaria*
(Received 19 August 2005; published 24 October 2005)

The analysis of the Raman scattering cross section of the radial breathing modes of double-wall carbon nanotubes allowed us to determine the optical transitions of the inner tubes. The Raman lines are found to cluster into species with similar resonance behavior. The lowest components of the clusters correspond well to sodium sodecyl sulfate wrapped high pressure carbon monoxide grown tubes. Each cluster represents one particular inner tube inside different outer tubes and each member of the clusters represents one well-defined pair of inner and outer tubes. The number of components in one cluster increases with the decreasing inner tube diameter and can be as high as 14 spread over 30 cm^{-1}. This suggests a lot of variation in the diameter difference of inner-outer tube pairs.

DOI: 10.1103/PhysRevB.72.161404 PACS number(s): 78.67.Ch, 63.20.Dj, 78.30.Na, 78.66.Tr

Double-wall carbon nanotubes (DWCNTs) are interesting structures in the family of carbon nanophases, especially when they are grown by the annealing of so-called peapods, i.e., single-wall carbon nanotubes (SWCNTs) filled with fullerenes.[1] The outer tubes diameter of such DWCNTs are of the same small size (around 1.4 nm) as it is typical for SWCNTs. This means, they provide the same spatial resolution for sensors or the same field enhancement for electron emitters as the latter but exhibit a higher stiffness. The inner tubes, with typical diameters of 0.7 nm, have a rather high curvature and are thus expected to exhibit significant deviations from graphene with respect to their mechanical and electronic properties. Amongst others, the electron-phonon coupling is expected to considerably increase as compared to graphene, which might result in superconductivity or a Peierls transition. Also, the concentric layers in the DWCNTs represent curved graphite sheets with an interesting van der Waals–type interaction and DWCNTs are well-defined model materials for multiwall CNTs. Finally, by filling SWCNTs with isotope labeled fullerenes it is possible to produce DWCNTs with ^{13}C enriched inner and normal ^{12}C outer tubes.[2]

The peapod-grown DWCNTs attracted additional interest as the inner tubes are grown in an highly unperturbed environment and thus exhibit unusual narrow lines for the radial breathing mode (RBM) Raman response.[3] In this sense, the inside of the outer tubes has been termed a "nano-cleanroom." Moreover, the Raman signal from the RBMs of the inner tubes exhibits strong resonance enhancement and the observed number of lines is larger than the number of geometrically allowed species.[4]

Similar to the outer tubes, the geometric and electronic properties of the inner tubes are uniquely determined by their chiral vectors (m,n), along which the graphene layers are rolled up into tubes.[5] Due to the quasi-one-dimensionality of the tubes, the electronic states are jammed into Van Hove singularities (VHSs). Recent experiments suggest that the optical transitions of semiconducting (E_{ii}^{S}) and metallic (E_{ii}^{M}) tubes arise from excitonic states close to the VHSs instead from the VHSs as such.[6] These transition energies scatter around lines with slopes proportional to the inverse tube diameter $1/D$. Refined calculations revealed considerable curvature corrections to the transition energies, especially for small diameter tubes.[7–9] Experimental information on these effects has recently been obtained from the Raman and luminescence measurements of HiPco (high pressure carbon monoxide grown) tubes with a mean diameter of about 1 nm.[10–12] The pattern of the deviation from the linear relation between E_{ii} and $1/D$ can be categorized into tube families with respect to $2m+n=\text{const}$. There are the metallic tubes with $2m+n \equiv 0 \pmod 3$ and two types of semiconducting tubes with $2m+n \equiv 1 \pmod 3$ (SI) and $2m+n \equiv 2 \pmod 3$ (SII). For the E_{22}^{S} transition, the SI tubes deviate strongly from the linear relation towards lower transition energies whereas the SII tubes exhibit a smaller deviation towards higher transition energies. In all cases zigzaglike tubes close to $(m,0)$ show the largest deviation from the linear relationship.

The RBM frequencies also scale roughly as $1/D$ and have therefore been used repeatedly for the structural analysis of SWCNTs, particularly with respect to the diameter distribution. By analyzing the Raman cross section of the RBMs it is possible to determine chiralities and electronic transition energies of CNTs.[11,12]

Here, we present the results of resonance Raman measurements in the RBM range of DWCNTs. These measurements unraveled the optical transitions of the inner tubes which cannot be accessed by optical and scanning probe experiments. Using a contour plot where the Raman cross section is plotted over a two-dimensional grid of RBM frequency and laser excitation energy, we found a well-expressed fine structure in the resonance pattern. An analysis of this pattern showed a clustering of the inner tubes RBMs near the HiPco transition energies and frequencies. The clusters start around the HiPco frequencies and extend up to 30 cm^{-1} to higher frequencies. They consist of up to 14 well-expressed components. Each cluster represents one particular inner tube inside different outer tubes and each member of the clusters represents a well-defined pair of one inner tube in one outer tube. Within one cluster, the transition energies

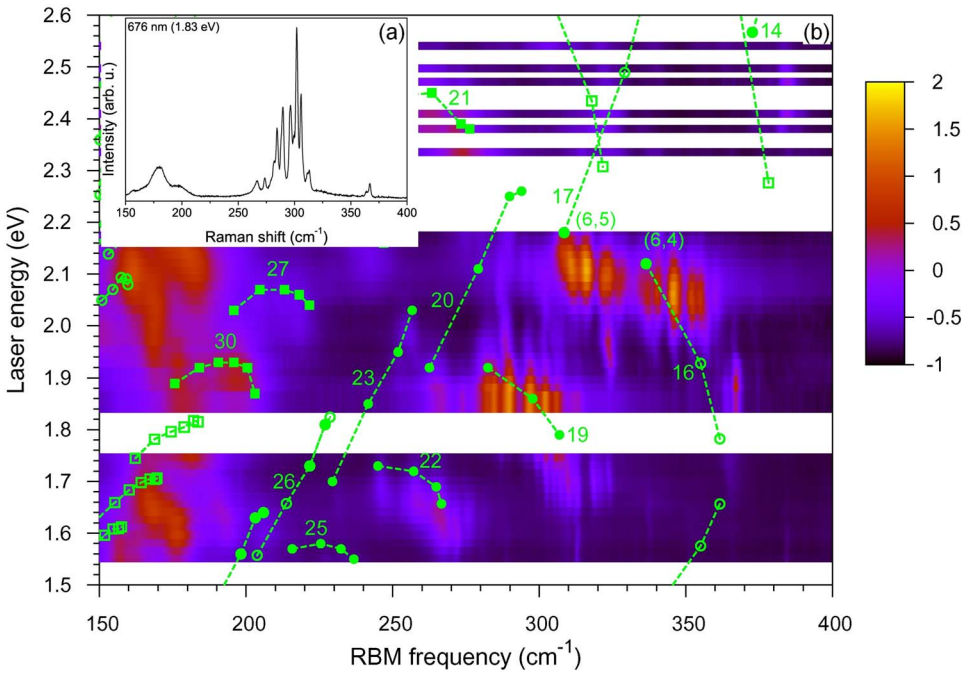

FIG. 1. (Color online) (a) Raman response of the RBM region of DWCNTs sample B. (b) Logarithm of the Raman cross section of the tubes as a function of laser energy and RBM frequency. Filled symbols are measured RBM frequencies and transition energies of sodium sodecyl sulfate (SDS) wrapped HiPco tubes averaged from Refs. 10–12 (circles and squares denote semiconducting and metallic tubes, respectively). Open symbols are extended tight-binding calculations (Ref. 7) corrected for many-body effects (Ref. 13). Tube families are connected with dashed lines and assigned by family numbers $2m+n=$const.

show a redshift of about 2 meV/cm^{-1}. We explain the existence of such "pair spectra" and the redshift of the transition energies by the interactions between the inner and outer tubes. This explanation is supported by model calculations.

The DWCNTs studied here were obtained by annealing C_{60} peapods at 1250 °C in a dynamic vacuum for 2 h.[1] Two samples with mean outer diameters of 1.39 nm (sample A) and 1.45 nm (sample B) were studied here. The Raman spectra for the measurement of the resonance cross section were recorded in backscattering geometry at ambient conditions using a Dilor XY triple spectrometer operated in normal resolution and a liquid N_2 cooled charge-coupled device detector. Selected spectra were measured in high resolution (HR) at 90 K. In this case, the resolution of the spectrometer was 0.5 cm^{-1} for red laser excitation. The spectra were obtained with different lasers such as an Ar/Kr, a Ti:sapphire, and a dye laser with Rhodamine 6G and Rhodamine 101. Excitation was between 1.54 and 2.54 eV (488 to 803 nm) with a spacing of about 15 meV in the red to yellow spectral region. The frequencies were corrected using calibration lamps. In order to determine Raman cross sections and to correct for the spectrometer and detector sensitivity, all spectra were normalized to the well-known cross section for the Si F_{1g} mode around 520 cm^{-1}.

Figure 1(a) depicts a typical Raman spectrum of DWCNTs in the frequency range of the RBM. The broad and structured line pattern around 180 cm^{-1} and the set of strong and narrow lines in the spectral range from 230 to 400 cm^{-1} originate from the outer and inner tubes, respectively. Figure 1(b) shows the color coded logarithm of the RBM Raman cross section of DWCNTs sample B as a function of laser energy and RBM frequency for normal spectrometer resolution. The broad band between 150 and 210 cm^{-1} is the response from the outer tubes. Between about 230 and 400 cm^{-1} one can observe the RBM response of the inner tubes. For this energy range, mainly the E_{22}^{S} (circles) and parts of the E_{11}^{M} transitions (squares) can be seen.

From the comparison with results for HiPco tubes one can easily identify the families 22, 19, and 16 in the SI branch of the E_{22}^{S} transition. Resonances from the SII tubes (families 23, 20, and 17) are, in general, weaker but can still be observed, especially the (6, 5) tube in family 17. The metallic transitions are also close to the HiPco results.

The RBMs of the inner tubes clearly show a clustering of components close to the HiPco transitions. The low frequency end of the clusters coincides well with the results from the HiPco tubes except for a downshift in energy of about 50 meV. For the (6, 4) inner tube in family 16 the total width of the cluster is about 30 cm^{-1}. The width of the clustered lines clearly decreases with increasing inner tube diameters. For the largest diameter inner tubes (family 22) almost no clustering is observed and results are in very good agreement with the response from the HiPco tubes.

A number of very intensive Raman lines are located close to the transitions of the isolated (6, 5) and (6, 4) tubes in families 17 and 16, respectively. The two tubes are well separated in frequency and the clusters can be well assigned to those tubes. In the following discussion we will, therefore, mainly refer to these tubes, although all results hold correspondingly for the other inner tubes. Within one cluster the peak resonances of the components are clearly shifted to lower energies with increasing frequency. For the (6, 5) and

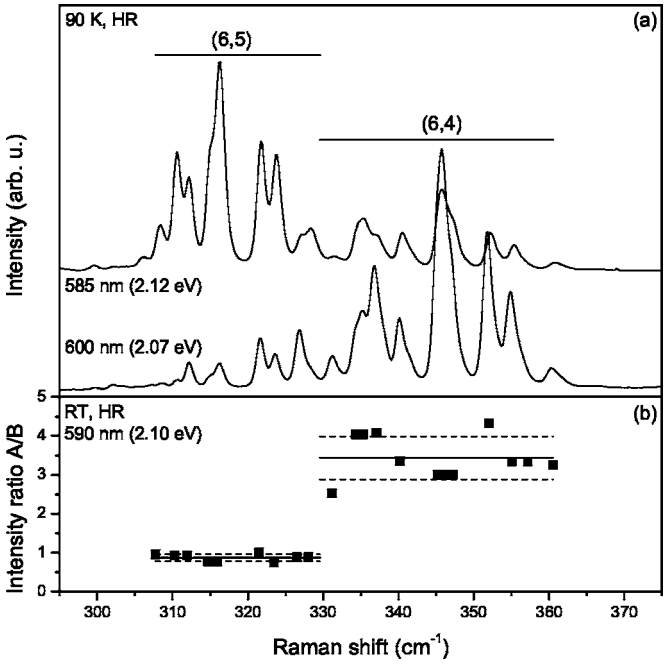

FIG. 2. (a) High resolution Raman response for the (6, 5) and (6, 4) inner tubes for sample A as excited with two different lasers. The horizontal lines cover the widths of the clusters. (b) Intensity ratio of the RBM components for the (6, 5) and (6, 4) tubes of samples A and B with small and large mean outer tubes diameters, respectively. The dashed lines indicate the standard deviation.

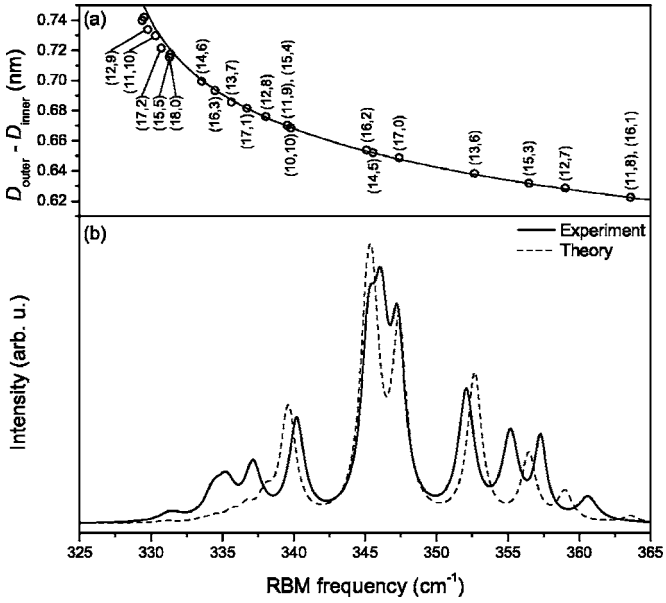

FIG. 3. (a) RBM frequency of a (6, 4) inner tube as a function of the diameter difference to various outer tubes (indicated by their chiral vectors). (b) Raman line pattern for the RBM of the (6, 4) inner tube as obtained from experiment (solid line) and from theory (dashed line) as described in the text.

(6, 4) cluster we get $-2.7(6)$ meV/cm^{-1} and $-0.9(4)$ meV/cm^{-1}, respectively. On the average, the shift is about -2 meV/cm^{-1}.

Two strong resonances at (322 cm^{-1}, 1.92 eV) and at (368 cm^{-1}, 1.86 eV) could not be assigned, although they were observed in all samples studied. The lower energy resonance may be related to the (7, 2) tube of family 16. The higher energy resonance could originate from (6, 5) with a nonsymmetric resonance transition.[14]

In order to demonstrate the clustering effect more clearly and to get some information on the number of components in the clusters, we measured the spectral range of the RBM for the (6, 5) and for the (6, 4) tubes in high resolution at low temperature [see Fig. 2(a)]. While for the lower energy laser all components of the (6, 4) species are in resonance the components of the (6, 5) tubes remain weak. For the higher energy laser the result is just the opposite. From a fit to the observed structures a total number of 9 and 14 components were found for the (6, 5) and the (6, 4) clusters, respectively.

To check the stability of the clustered components in the spectra we compared the patterns for two samples with different outer tube diameters. As Fig. 2(b) shows, the (6, 4) cluster is about a factor 3.4 stronger in intensity in sample A (1.39 nm) than in sample B (1.45 nm). The intensity of the (6, 5) components in sample A is only about 87% of that in sample B. This is as expected, since within the smaller diameter outer tubes proportionally more smaller inner tubes grow.[15]

The crucial result that a rather large number of peaks in the RBM range of the Raman spectra have the same resonance behavior is surprising. It strongly suggests that all components of one cluster originate from the same inner tube. This means the inner tubes can be accommodated in a rather large number of different outer tubes and the wall to wall distance can be quite different from its optimum value.[16] Thus, the clustered lines represent pair spectra of one inner tube inside several well-defined outer tubes.

Figure 3(a) depicts the calculated upshift of the RBM frequency of a (6, 4) inner tube as a function of the diameter difference to various outer tubes. In the calculations we considered the tubes as elastic continuum cylinders interacting with each other with a Lennard-Jones (LJ) potential parametrized for graphite.[17] The relaxed structure of the DWCNTs was found by minimization of the total energy E equal to the sum of the elastic energies of both tubes and the inter tube interaction energy E_{LJ}, $E=Y_1\pi[R_{\mathrm{i}}(\Delta R_{\mathrm{i}}/R_{\mathrm{i}})^2+R_{\mathrm{o}}(\Delta R_{\mathrm{o}}/R_{\mathrm{o}})^2]+E_{\mathrm{LJ}}$. Here R_{i} and R_{o} are the inner and outer tube radii, ΔR_{i} and ΔR_{o} are their changes, $Y_1=Yd$, $Y=1.06$ TPa is the graphene in-plane Young's modulus, and $d=0.335$ nm is the tube wall thickness. Compared with the continuum model results,[4] the frequency upshift for small diameter differences became slightly smaller.

In Fig. 3(b) the solid line is the experimental spectrum of sample A obtained in HR at 90 K where the intensity of each component was normalized to its measured maximum cross section. The spectrum thus shows the population distribution of the inner-outer tube pairs. The calculated spectrum [dotted line in Fig. 3(b)] was obtained by assigning a Lorentzian to each calculated frequency whose intensity was for simplicity assumed to be determined by a Gaussian distribution. This procedure anticipates equal resonance matrix elements for all members of a cluster, which is certainly well justified. The calculated frequencies were scaled with a factor 0.98. To

get the best agreement between theory and experiment, the parameters of the Gaussian were $\omega_0=348.9$ cm^{-1} and $\sigma=5.2$ cm^{-1}. For the intermediate frequencies, experiment and theory are in good agreement. For lower and higher frequencies, the components deviate from the experiment. The maximum of the simulated spectrum is found for a diameter difference of about 0.66 nm, which is smaller than the experimental value of 0.72 nm reported in Ref. 18. This shows that the LJ potential must be reparametrized for the curved sp^2 networks of DWCNTs.

The frequency upshift and the transition energy downshift within one cluster can be understood from an increasing interaction between the two shells for decreasing diameter difference. This interaction acts on the inner shell like a radial pressure. The pressure dependence of E_{22} for the (6, 4) and the (6, 5) inner tubes was calculated in the extended tight-binding framework.[7] The corresponding values are −7.8 meV/GPa and −2.5 meV/GPa. After Ref. 19 the frequencies shift with about 1.1 cm^{-1}/GPa. Thus one gets −7.1 meV/cm^{-1} and −2.3 meV/cm^{-1}, respectively. The signs and the order of magnitude compare well with the experiment. Additionally, from the measured pressure induced shift of the E_{22}^S transition[20] for a (6, 5) tube of −4 meV/GPa one gets −3.6 meV/cm^{-1}, which is very close the experimental value of −2.7 meV/cm^{-1}.

In summary, we report on the optical transitions of very high curvature SWCNTs accommodated inside host outer tubes as derived from their resonance Raman cross section. The observed Raman lines are clustered and represent pair spectra between one inner tube and several well-defined outer tubes. The number of components in the cluster increases with decreasing tube diameter. The leading edges of the clusters correspond to the HiPco tubes with respect to frequency and transition energy except for a redshift of 50 meV. Additional redshifts of about 2 meV/cm^{-1} within a cluster are understood from a radial pressure generated by different outer tubes. These results now provide a unified picture for the high curvature nanotubes from the HiPco process and from the DWCNTs species.

Valuable discussions with A. Jorio, A. Rubio, and L. Wirtz are gratefully acknowledged. Work was supported by FWF Project No. P17345, Marie-Curie Project Nos. MEIF-CT-2003-501099 and MEIF-CT-2003-501080, and by NATO CLG 980422.

[1] S. Bandow, M. Takizawa, K. Hirahara, M. Yudasaka, and S. Iijima, Chem. Phys. Lett. **337**, 48 (2001).

[2] F. Simon, C. Kramberger, R. Pfeiffer, H. Kuzmany, V. Zólyomi, J. Kürti, P. M. Singer, and H. Alloul, Phys. Rev. Lett. **95**, 017401 (2005).

[3] R. Pfeiffer, H. Kuzmany, C. Kramberger, C. Schaman, T. Pichler, H. Kataura, Y. Achiba, J. Kürti, and V. Zólyomi, Phys. Rev. Lett. **90**, 225501 (2003).

[4] R. Pfeiffer, C. Kramberger, F. Simon, H. Kuzmany, V. N. Popov, and H. Kataura, Eur. Phys. J. B **42**, 345 (2004).

[5] S. Reich, C. Thomsen, and J. Maultzsch, *Carbon Nanotubes* (Wiley-VCH, Weinheim, 2004).

[6] F. Wang, G. Dukovic, L. E. Brus, and T. F. Heinz, Science **308**, 838 (2005).

[7] V. N. Popov, New J. Phys. **6**, 17 (2004).

[8] V. N. Popov and L. Henrard, Phys. Rev. B **70**, 115407 (2004).

[9] G. G. Samsonidze, R. Saito, N. Kobayashi, A. Grüneis, J. Jiang, A. Jorio, S. G. Chou, G. Dresselhaus, and M. S. Dresselhaus, Appl. Phys. Lett. **85**, 5703 (2004).

[10] S. M. Bachilo, M. S. Strano, C. Kittrell, R. H. Hauge, R. E. Smalley, and R. B. Weisman, Science **298**, 2361 (2002).

[11] C. Fantini, A. Jorio, M. Souza, M. S. Strano, M. S. Dresselhaus, and M. A. Pimenta, Phys. Rev. Lett. **93**, 147406 (2004).

[12] H. Telg, J. Maultzsch, S. Reich, F. Hennrich, and C. Thomsen, Phys. Rev. Lett. **93**, 177401 (2004).

[13] A. Jorio, C. Fantini, M. A. Pimenta, R. B. Capaz, G. G. Samsonidze, G. Dresselhaus, M. S. Dresselhaus, J. Jiang, N. Kobayashi, A. Grüneis, and R. Saito, Phys. Rev. B **71**, 075401 (2005).

[14] A. Grüneis, R. Saito, J. Jiang, G. G. Samsonidze, M. A. Pimenta, A. Jorio, A. G. Souza Filho, G. Dresselhaus, and M. S. Dresselhaus, Chem. Phys. Lett. **387**, 301 (2004).

[15] F. Simon, Á. Kukovecz, C. Kramberger, R. Pfeiffer, F. Hasi, H. Kuzmany, and H. Kataura, Phys. Rev. B **71**, 165439 (2005).

[16] A. Hashimoto, K. Suenaga, K. Urita, T. Shimada, T. Sugai, S. Bandow, H. Shinohara, and S. Iijima, Phys. Rev. Lett. **94**, 045504 (2005).

[17] J. P. Lu, X.-P. Li, and R. M. Martin, Phys. Rev. Lett. **68**, 1551 (1992).

[18] M. Abe, H. Kataura, H. Kira, T. Kodama, S. Suzuki, Y. Achiba, K.-i. Kato, M. Takata, A. Fujiwara, K. Matsuda, and Y. Maniwa, Phys. Rev. B **68**, 041405(R) (2003).

[19] U. D. Venkateswaran, D. L. Masica, G. U. Sumanasekera, C. A. Furtado, U. J. Kim, and P. C. Eklund, Phys. Rev. B **68**, 241406(R) (2003).

[20] J. Wu, W. Walukiewicz, W. Shan, E. Bourret-Courchesne, J. W. Ager III, K. M. Yu, E. E. Haller, K. Kissell, S. M. Bachilo, R. B. Weisman, and R. E. Smalley, Phys. Rev. Lett. **93**, 017404 (2004).